Two-level model and the dynamic Hall effect in nonlinear semiconductors

Shwu-Yun Tsay Tzeng[1,*] and Yi-Chen Cheng[2]
[1]*Department of Electro-Optical Engineering, National Taipei University of Technology, Taipei, Taiwan 106, Republic of China*
[2]*Department of Physics, National Taiwan University, Taipei, Taiwan 106, Republic of China*
(Received 24 October 2002; revised manuscript received 24 February 2003; published 30 July 2003)

Nonlinear transport properties of a semiconductor with an S-shaped negative differential conductivity is usually described by the well-established two-impurity-level model. However, previous attempts in using the two-impurity-level model to explain the observed dynamic Hall effect in nonlinear semiconductors failed, at least in the spatially homogeneous case. The model predicts a stable state when the transverse magnetic field B is zero, and as B increases to exceed a critical value, the system undergoes limit cycle oscillations, but no further bifurcation no matter how large B is. Experimentally it was observed that n-GaAs with shallow impurities at 4.2 K exhibits limit cycle oscillations when the static electric field E_0 exceeds a critical value with $B=0$. When the applied transverse magnetic field B increases from 0 to about 100 mT, the system undergoes several bifurcation routes to chaos as E_0 increases. In this paper we establish a two-impurity-level model, with the assumption of spatial homogeneity, to explain the observed dynamic Hall effect in n-GaAs at 4.2 K. The dynamic behavior of our model has the main features of the experimental observations described in the above.

DOI: 10.1103/PhysRevB.68.035211 PACS number(s): 72.20.Ht, 47.52.+j

I. INTRODUCTION

It is well known that a semiconductor with an S-shaped current density-field (J-E) characteristic will exhibit many interesting nonlinear effects, such as displaying a hysteresis loop in the current-voltage (I-V) curve,[1,2] formation of current filaments[3,4], self-sustained oscillations and chaos,[2,5–10] when the system is connected in series with only a dc bias voltage. Many of the above nonlinear transport properties can be described by the well-established two-impurity-level model.[2] However, up to now, this two-level model, with the assumption of spatial homogeneity, fails to explain experimentally observed dynamic Hall effect when a transverse magnetic field B is applied to n-GaAs at helium temperatures.[11] The main feature of the experimental result is that, when $B=0$ the system exhibits limit cycle oscillations, and as B increases up to 100 mT, the system generates a sequence of quasiperiodic and frequency-locking current oscillations and finally a Ruelle-Takens-Newhouse scenario to chaos. In 1991, Hüpper and Schöll[12] proposed a one-level model to simulate the dynamic Hall effect. Their main result is that, when $B=0$ the system is always stable irrespective of the value of the applied electric field. As B exceeds a critical value, the system undergoes period-doubling routes to chaos, and type-I intermittency. However, this is a *one*-level model and the corresponding physical system is not a *nonlinear* semiconductor, because the model exhibits positive differential conductivity (PDC) for all values of the electric field E in the current density J vs electric field E curve. This is to be compared with a nonlinear semiconductor which possesses negative differential conductivity (NDC) for some range of E. The PDC system is stable for all values of the applied electric field E when $B=0$. In 1992 the same authors[13,14] extended the theoretical analysis to include the two-level model with spatial homogeneity. They used two different sets of material parameters for the two-level model to obtain two different oscillation mechanisms: (1) self-generated oscillations and chaos without a magnetic field, the system undergoes period-doubling routes to chaos with $B=0$ and (2) magnetic field induced limit cycle oscillations when B exceeds a critical value. We have checked the calculations to confirm that the dynamic behavior does not change when a transverse magnetic field B is applied to case (1), only the bifurcation point (value of the applied electric field) is shifted. For case (2), we take the same parameters listed in Ref. 13 and follow the simulation proposed by the authors. The system is stable when $B=0$, and as the magnetic field B increases beyond a critical value the system undergoes limit cycle oscillations no matter how large B is. Therefore the proposed two-level models are unable to explain the observed dynamic Hall effect.[11] Neither case (1) nor case (2) is close to the experimental observations.

In this paper we would like to propose a two-level model, with the assumption of spatial homogeneity, to explain the observed dynamic Hall effect in n-GaAs with shadow impurities at helium temperatures.[11] The governing dynamic equations are basically the same as previous models, except that we use a set of slightly different parameter values which are more appropriate for shadow impurities in n-GaAs. We also take into account the magnetic field effects in the impact ionization parameters as well as the energy level splitting between the impurity level and the conduction band. This is because the conduction electron effective mass of n-GaAs is rather small ($\approx 0.066\mathrm{m}_0$), thus the Landau level shift of the conduction electrons is much larger than the Zeeman shift of the bound impurity electrons which may have important effects in the impact ionization processes. The main result of our model is that, when there is no magnetic field $B=0$, the system undergoes limit cycle oscillations when the applied electric field exceeds a critical value, and no further bifurcation is found as long as $B=0$. When a transverse magnetic field B is applied, the system undergoes period-doubling routes to chaos as B increases from 0 to exceed a critical value. Our theory predicts the main features of the experimental observations: there are only limit cycle oscillations when $B=0$, and as B increases from 0 to exceed a critical

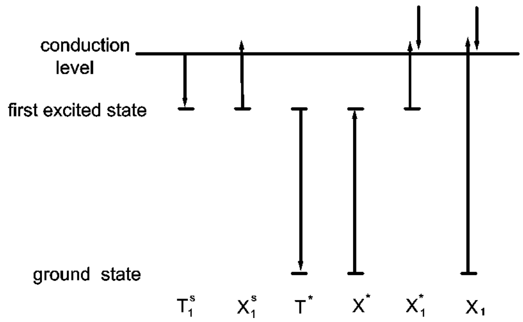

FIG. 1. Generation-recombination process considered in the two-level model, involving the conduction band, the trap ground state and the first excited state.

value, the system undergoes various routes to chaos.

II. THE MODEL

Consider an n-type semiconductor with the donor concentration N_D and the acceptor concentration N_A ($N_D \gg N_A$), and the effective doping concentration $N_D^* = N_D - N_A$. The two-level model considers the electronic states of a donor impurity consisting of two levels: the ground and the first excited state. An electron in these states can be thermally ionized or impact ionized to the conduction band, and then recombines with a donor having an empty state. This is known as the generation-recombination (GR) processes. Denote the electron densities as n, n_{t_1}, and n_{t_2} for the conduction band, the donor ground state and the first excited state, respectively. The GR rate equations are given by[2,6]

$$\dot{\nu} = X_1 N_D^* \nu \nu_{t_1} + (X_1^s + X_1^* N_D^* \nu)\nu_{t_2} - T_1^s N_D^* (N_A/N_D^* + \nu)\nu, \tag{1}$$

$$\dot{\nu}_{t_1} = -(X^* + X_1 N_D^* \nu)\nu_{t_1} + T^* \nu_{t_2}, \tag{2}$$

where $\nu = n/N_D^*$, . . . , etc., and ν_{t_2} can be eliminated by the condition of the conservation of charge $\nu_{t_2} = 1 - \nu - \nu_{t_1}$. The parameters X_1^s, T_1^s, X_1, X_1^*, X^*, and T^* denote the appropriate GR coefficients as shown in Fig. 1. The forms of the GR coefficients and how the presence of a magnetic field will affect them, will be discussed in the next section.

Equations (1) and (2) are two of the dynamic equations, other dynamic equations are obtained from the circuit equations. We consider the case that a static electric field is applied in the x direction $\boldsymbol{E}_0 = E_0 \hat{\boldsymbol{x}}$ and a static magnetic field in the y direction $\boldsymbol{B} = B\hat{\boldsymbol{y}}$, then in the limit of a very large resistance, we have the dynamic equations for the n-type semiconductors[12,15]

$$\epsilon \dot{E}_x = J - e\nu N_D^* \mu_B v_x - e\nu N_D^* \mu \mu_B B v_z, \tag{3}$$

$$\epsilon \dot{E}_z = e\nu N_D^* \mu \mu_B B v_x - e\nu N_D^* \mu_B v_z, \tag{4}$$

$$\epsilon \dot{E}_y = -e N_D^* \mu E_y. \tag{5}$$

Here $\nu N_D^* = n$ is the conduction electron density, J the total current density, ϵ the permittivity of the sample, μ the conduction electron mobility at zero magnetic field, $\mu_B = \mu/(1+\mu^2 B^2)$, and v_x, v_z are, respectively, the x and z component of the drift velocity $\boldsymbol{v}$ of the conduction electrons. We will give the explicit forms of v_x and v_z in the next section. Apparently, E_y is decoupled from E_x and E_z, and the solution of E_y decreases exponentially to zero. For small perturbations about the fixed point, Eqs. (1)–(4) are then the four basic dynamic equations we have to solve for the transverse magnetic field case, i.e., the dynamic Hall effect. The applied electric field E_0 is chosen as the control parameter. E_0 is related to the static state total current density J in Eq. (3) $J = J_0 = en(\boldsymbol{E}^0)v_x(\boldsymbol{E}^0)$ in the steady state, when all the quantities in the left-hand side of Eqs. (1)–(4) are zero. In a steady state $\boldsymbol{E}^0 = (E_0, 0, E_z^0)$, E_0 is the applied electric field, and E_z^0 is the induced static Hall field. Therefore E_0 is the x component of the electric field for the fixed point of the dynamic equations (1)–(4).

III. MAGNETIC FIELD EFFECT ON THE GR COEFFICIENTS

In the absence of a magnetic field, the impact-ionization coefficients X_1 and X_1^* (see Fig. 1) can be approximated as[16]

$$X_1(E) = X_1^0 e^{-\varepsilon_b/E}, \tag{6}$$

$$X_1^*(E) = X_1^{*0} e^{-\varepsilon_b^*/E}, \tag{7}$$

where E is the total electric field, ε_b and ε_b^* are the impurity ground and the first excited state binding energy, respectively. When a transverse magnetic field B is applied to the system, there will be two effects on X_1 and X_1^*. The first one is the binding energy shift of ε_b and ε_b^* due to the Landau level shift of the conduction electrons. Because the conduction electron effective mass $m^* \approx 0.066 m_0$ of n-GaAs is much less than the rest mass m_0, the Zeeman shift of the bound electrons may be neglected. The second one is the enhancement of the cross sections of the impact-ionization coefficients X_1 and X_1^* due to the magnetic field.[17] The conduction electrons with larger drift velocities make more contributions to the impact-ionization cross sections. For these electrons the Lorentz force is not completely cancelled by the electric force of the Hall field, and therefore their orbits are helical rather than linear. The radius of the orbit is smaller for an electron with a larger velocity. This implies that electrons with larger velocity will move with a slower translational velocity, because the magnitude of the velocity of an electron is not altered by the magnetic field. These electrons are therefore much easier to be attracted by a nearby impurity site and increase the probability of impact ionization. Combining these two effects, the impact ionization coefficients X_1 and X_1^* can be written as

$$X_1(E,B) = X_1^0 (1 + \gamma \mu B) e^{-\varepsilon_b^B/E}, \tag{8}$$

$$X_1^*(E,B) = X_1^{*0} (1 + \gamma' \mu B) e^{-\varepsilon_b^{*B}/E}, \tag{9}$$

where γ and γ' are adjustable parameters. Referring to Ref. 17 we take $\gamma=0.1$ and $\gamma'=0.4$. In the presence of a transverse magnetic field, the z-component of the electric field E_z will be nonzero and therefore $E=(E_x^2+E_z^2)^{1/2}$ is the total electric field. Because the Zeeman shifts are much smaller and much more complicated than the Landau level shift, we take into account only the Landau level shift to simplify the calculations. The magnetic field dependent binding energies ε_b^B and ε_b^{*B} then have the form

$$\varepsilon_b^B=\varepsilon_b+\Delta\varepsilon_B, \tag{10}$$

$$\varepsilon_b^{*B}=\varepsilon_b^*+\Delta\varepsilon_B, \tag{11}$$

where $\Delta\varepsilon_B=\hbar\omega_c^*/2$ $(\omega_c^*=eB/m^*c)$ is the conduction ground state Landau level shift. For n-GaAs $m^*=0.066m_0$, $\Delta\varepsilon_B=0.877B$ meV with B in units of T (Tesla). The energy shift $\Delta\varepsilon_B$ can not be neglected for B close to a few tenths of 1 T, as $\varepsilon_b=6.0$ meV and $\varepsilon_b^*=1.5$ meV for n-GaAs.

Magnetic field effect on the binding energies of the impurity electrons will also affect the thermal ionization probability of the impurity electrons at low temperatures. Taking into account the effect of the Boltzmann factor we may write the thermal ionization coefficient as

$$X_1^s(B)=X_1^s(0)e^{-\Delta\varepsilon_B/k_BT}, \tag{12}$$

where k_B is the Boltzmann constant. At helium temperature $T=4.2$ K, $k_BT=0.362$ meV which is comparable to $\Delta\varepsilon_B$ for B to be a few tenths of 1 T.

Finally the components of the drift velocity are modeled by the phenomenological saturation form[18] modified by the presence of the magnetic field

$$v_x=\frac{\arctan(r_BE_x)}{r_B} \tag{13}$$

and

$$v_z=\frac{\arctan(r_BE_z)}{r_B}, \tag{14}$$

where $r_B=r/(1+\mu^2B^2)$ and r is a dimensionless saturation parameter for $B=0$. This form of saturation drift velocity has been used in several two-level model calculations.[2,13,19]

IV. NUMERICAL RESULTS AND CONCLUSIONS

In this section we present the results of numerical simulations for the two-level model with a transverse magnetic field by using the parameter values which are appropriate for n-GaAs at $T=4.2$ K. The dynamic equations are Eqs. (1)–(4) with the magnetic field dependent GR parameters Eqs. (8)–(12) and the drift velocity components Eqs. (13)–(14). The effective doping concentration N_D^* is taken to be 1.0×10^{15} cm^{-3}, and other parameter values are listed in Table I. The four dynamic variables are (ν,ν_{t_1},E_x,E_z). The control parameter is the applied electric field E_0, and the transverse magnetic field B is considered to be an adjustable parameter. This means that we choose a value of B and study the dynamic behavior of the dynamic equations (1)–(4) as the control parameter E_0 varies. By choosing different values of B and repeating the calculations, we can study the magnetic field effect on the bifurcation features of the dynamic system. We use the standard procedure to study the dynamic behavior of the system. We first solve the fixed point of the dynamic equations (1)–(4), when all the time derivatives in the left-hand side of these equations are zero. As we analyze the eigenvalues of a steady state, we linearize the dynamic equations around the fixed point and solve the eigenvalue problem of the Jacobian matrix of the linearized dynamic equations. There are four eigenvalues. We are interested in the case where there are two real and negative eigenvalues, and the other two are complex conjugate to each other. The nonlinear oscillations of the electron density and the electric field are found when the real part of the complex eigenvalues are *positive*. This can be found only when the system is operating in the NDC regime.

In Fig. 2 we plot the real part of the complex eigenvalues

TABLE I. The parameter values for n-type GaAs at 4.2 K for the two-level generation-recombination model studied in this paper.

Parameter	Value
$T_1^sN_D^*\tau$	10^{-2}
$T^*\tau$	10^{-5}
$X_1^s\tau$	2×10^{-6}
$X^*\tau$	2×10^{-7}
$X_1^0N_D^*\tau$	5×10^{-4}
$X_1^{*0}N_D^*\tau$	10^{-2}
N_A/N_D^*	0.3
r	1.3
ϵ	$10\epsilon_0$
m^*	$0.066m_0$
μ	8×10^3 cm^2/V s

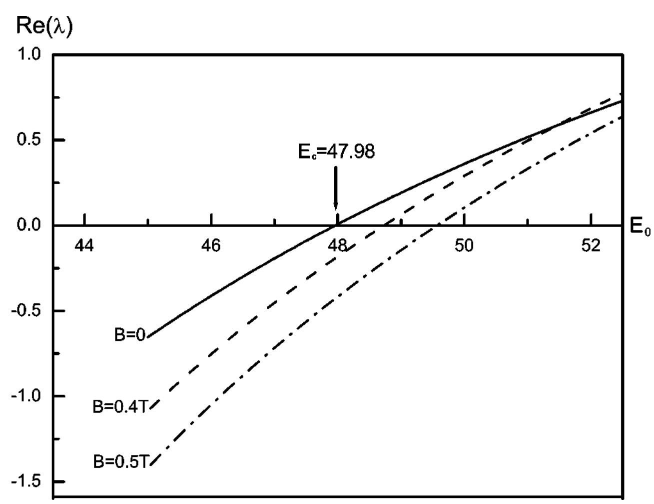

FIG. 2. The real part of the complex eigenvalue λ of the Jacobian matrix as a function of the control parameter E_0, for $B=0$, 0.4, and 0.5 T. Re(λ) is in units of $10^{-5}\tau^{-1}$ ($\tau=6.91\times10^{-13}$ sec is the relaxation time at $B=0$) and E_0 is in units of V/cm. The critical field E_c is the value of E_0 when Re(λ)$=0$.

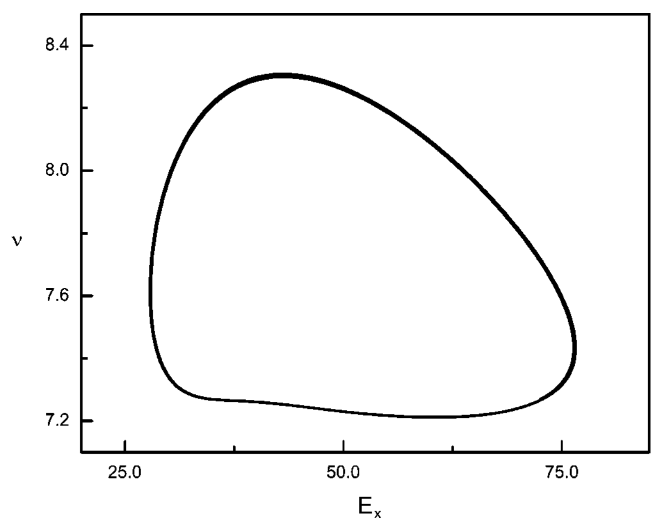

FIG. 3. The limit cycle oscillation in the (ν, E_x) plane with the magnetic field $B=0$ and control parameter $E_0=53.2$ V/cm. The conduction electron concentration ν is in units of $10^{-3}N_D^*$ and E_x is in units of V/cm.

λ as a function of the control parameter E_0 for three different values of the magnetic field B. We are interested in the region where Re(λ) changes sign from negative to positive as the control parameter E_0 increases. The critical field E_c, where Re(λ)=0, is 47.98 V/cm when $B=0$. The critical field E_c increases as B increases. For $E_0 > E_c$ the system undergoes a limit cycle oscillation for $0 \leqslant B < 0.1$ T. Only period one limit cycle can be found in this magnetic field range. The limit cycle oscillation of the conduction electron density ν vs E_x is plotted in Fig. 3 for the case $B=0$. As the magnetic field increases to the range 0.1 T$<B<$0.2 T, period two oscillations are found with a critical field $E_c=51.4$ V/cm. For $B>0.2$ T the system undergoes a series of period-doubling routes to chaos as the control parameter E_0 increases beyond the critical field E_c. We have found period-four and period-eight oscillations, but with further increase of E_0 the oscillations become nonperiodic and random which is a sign of chaos. The details of the phase portrait are shown in Figs. 4 and 5. Figures 4(a)–4(d) show, respectively, the projection of the phase portrait in the (ν, E_x) plane for period 1, period 2, period 4 and chaos for $B=0.5$ T. Figures 5(a)–5(b) show the projection of the phase portrait for period 4 in

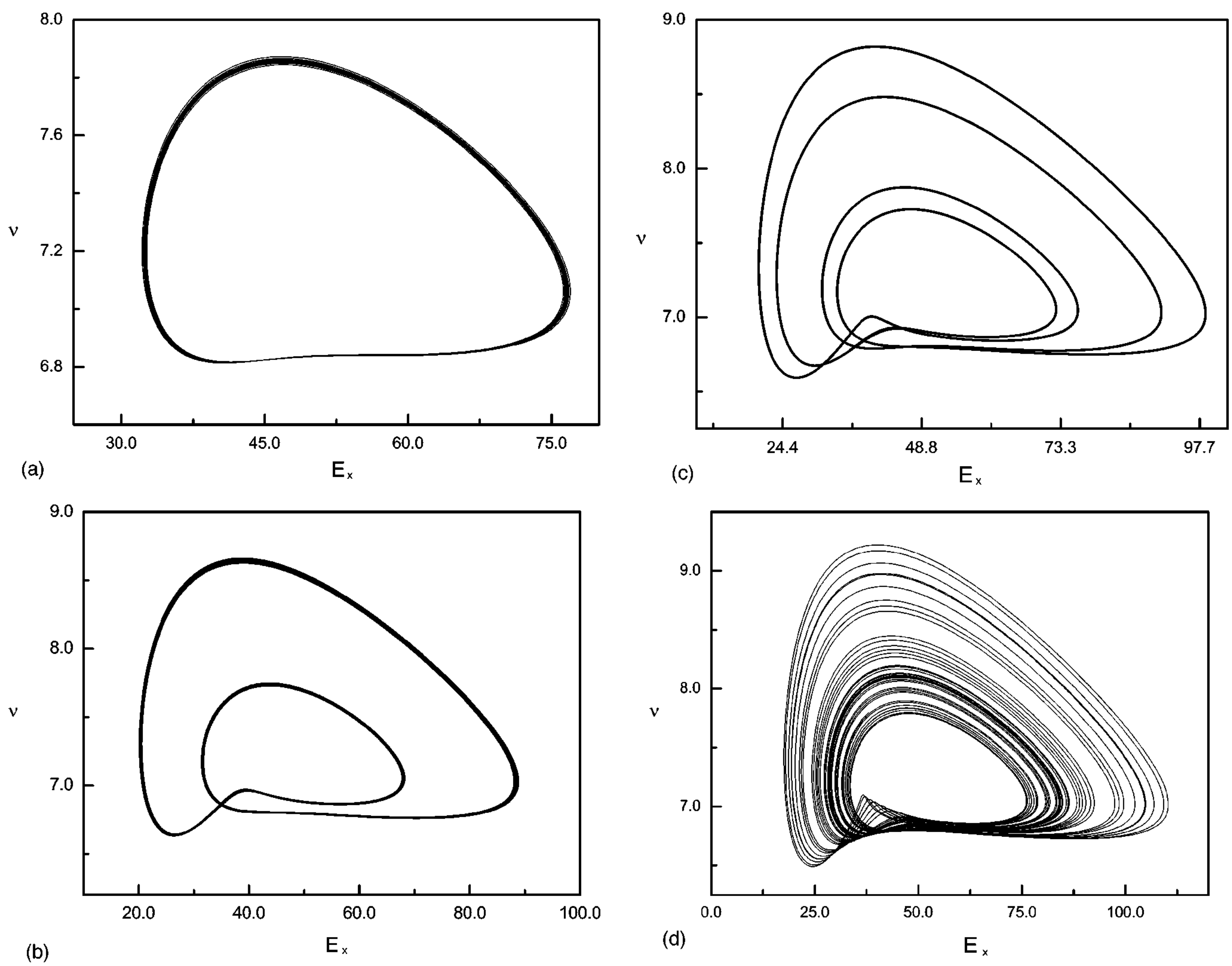

FIG. 4. The projection of the phase portrait in the (ν, E_x) plane with $B=0.5$ T, and the control parameter has the value (a) 52.0 (a limit cycle), (b) 53.2 (period-2 oscillation), (c) 53.78 (period-4 oscillation), and (d) 54.0 (chaos). The units are the same as in Fig. 3.

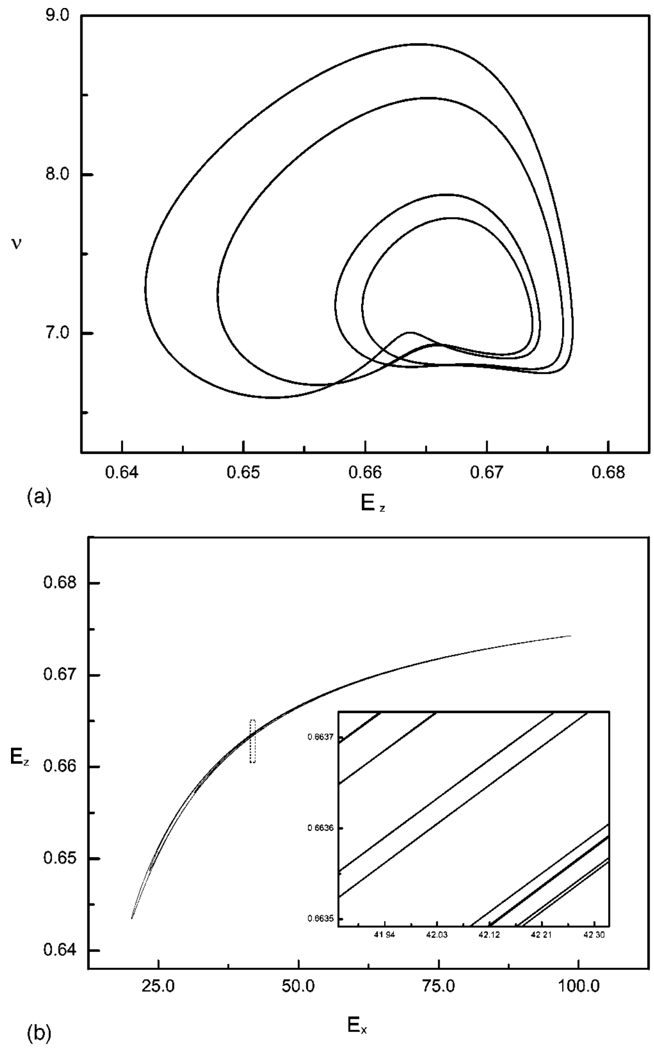

FIG. 5. The projection of the phase portrait in the (ν, E_z) plane (a), and in the (E_z, E_x) plane (b), with $B = 0.5$ T and the control parameter $E_0 = 53.78$. The units are the same as in Fig. 3.

the (ν, E_z) plane and the (E_z, E_x) plane, respectively. From Fig. 5(b) we see that the induced time dependent transverse electric field E_z varies almost linearly with the longitudinal field E_x. To see the dependence more clearly, an inset, which enlarges the dotted region, is shown in Fig. 5(b). A period-4 characteristic is clearly shown in the inset.

To summarize the magnetic field effect on the nonlinear behavior of *n*-GaAs we plot the bifurcation diagrams in Figs. 6 and 7. In Fig. 6, $E_x^{\max}$ is plotted as a function of the control parameter E_0 with $B = 0.5$ T, where $E_x^{\max}$ is the maximum value of the longitudinal electric field E_x. A period-doubling route to chaos is clearly shown in the figure. The dynamic behavior of the system is a function of both the transverse magnetic field B and the applied electric field E_0, a phase diagram is plotted in the (B, E_0) plane in Fig. 7. From this figure we can easily determine the dynamic behavior of the system for a given set of the control parameters (B, E_0). For example, if there is no magnetic field, i.e., $B = 0$, the system can only be a static normal system (for $E_0 < 47.98$ V/cm) or a limit cycle oscillation (for $E_0 > 47.98$ V/cm). When B is in

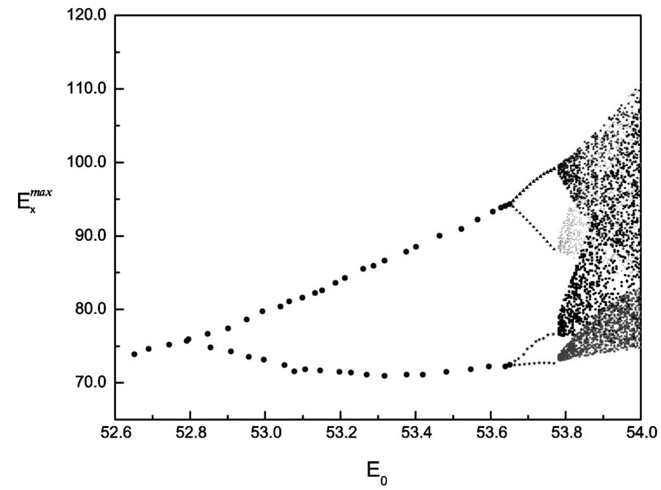

FIG. 6. Bifurcation diagram of the electric field maxima $E_x^{\max}$ vs the control parameter E_0, for the magnetic field $B = 0.5$ T. Both $E_x^{\max}$ and E_0 are in units of V/cm. This clearly shows a period-doubling route to chaos.

the range $0.1\ \mathrm{T} < B < 0.2\ \mathrm{T}$, the system can bifurcate to period-2 oscillations when E_0 exceeds a critical field $E_c^{(2)}$. $E_c^{(2)}$ decreases as B increases in the magnetic field range $0.1\ \mathrm{T} < B < 0.2$ T. But $E_c^{(2)}$ increases as B increases for $B > 0.2$ T. When $B > 0.2$ T period-4 oscillations come in, and then a small change of the control parameter E_0, the system will bifurcate to chaos via the period-doubling route.

In conclusion, we have established a spatially homogeneous two-level model to simulate the dynamic Hall effect which has been observed experimentally[11] for *n*-GaAs at 4.2 K. Our model predicts the main features of the experimental results. When there is no magnetic field, i.e., $B = 0$, the system can have limit cycle oscillations but no further bifurcation to more complicated oscillations. When the applied transverse magnetic field B exceeds a critical value, the sys-

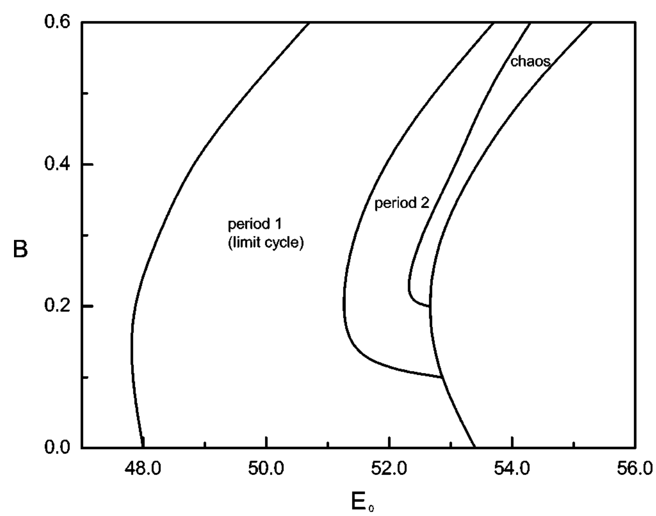

FIG. 7. Phase diagram in the (B, E_0) plane with E_0 in units of V/cm and B in units of T. For $B = 0$ the system can have only limit cycle oscillations. As B increases the system can undergo period-doubling route to chaos for large enough E_0.

tem may undergo various routes to chaos. Previous studies of the spatially homogeneous two-level models failed to predict the above two main features, either there are no oscillations when $B=0$ and only limit cycle oscillations when B exceeds a critical value, or the system may undergo various routes to chaos even without the applied magnetic field. In the latter case, the application of a transverse magnetic field does not alter the bifurcation features of the system, only the critical field E_c is shifted to higher values. Our model is essentially the same as previous models, except that we take into account the smallness of the effective mass of the conduction electrons in *n*-GaAs, which makes the Landau level shift of the conduction electrons non-negligible. Magnetic field effect on generation-recombination coefficients are also introduced. Without any modification on Landau level and generation-recombination parameters in our simulation, the system undergoes limit cycle oscillations, but does not undergo any further bifurcations even though B increases. Our model still has some discrepancies in comparing with the experimental result, which has much more complicated routes to chaos than the result of our theory. We think it may need a spatially inhomogeneous model to be in good agreement with the experiment. This will be our next project. There are several inhomogeneous calculations for related situations in the literature,[20–23] which may be helpful in constructing the model. However, before such a model is available, our simple spatially homogeneous model may provide a first step toward that goal.

*Electronic address: sytsay@ntut.edu.tw

[1] K. Aoki, T. Kondo and Watanabe, Solid State Commun. **77**, 91 (1991).
[2] E. Schöll, *Nonequilibrium Phase Transitions in Semiconductors* (Springer, Berlin, 1987).
[3] K. Kardell *et al.*, J. Appl. Phys. **64**, 1 (1988).
[4] F.S. Lee and Y.C. Cheng, Chin. J. Phys. (Taipei) **38**, 155 (2000).
[5] R. Obermaier, W. Böhm, W. Prettl, and P. Dirnhofer, Phys. Lett. **105A**, 149 (1984).
[6] E. Schöll, Physica B **134**, 271 (1985).
[7] E. Schöll, J. Parisi, B. Röhricht, J. Peinke, and R.P. Huebener, Phys. Lett. A **119**, 419 (1987).
[8] M. Weispfenning, I. Hoeser, W. Böhm, W. Prettl, and E. Schöll, Phys. Rev. Lett. **55**, 754 (1985).
[9] K. Aoki, T. Kobayashi, and K. Yamamoto, J. Phys. Soc. Jpn. **51**, 2373 (1982).
[10] K. Aoki and K. Yamamoto, Phys. Lett. **98A**, 72 (1983).
[11] J. Spangler, A. Brandl, and W. Prettl, Appl. Phys. A: Solids Surf. **48**, 143 (1989).
[12] G. Hüpper and E. Schöll, Phys. Rev. Lett. **66**, 2372 (1991).
[13] G. Hüpper, E. Schöll, and A. Rein, Mod. Phys. Lett. B **6**, 1001 (1992).
[14] E. Schöll, G. Hüpper, and A. Rein, Semicond. Sci. Technol. **7**, B480 (1992).
[15] R.A. Smith, *Semiconductors* (Cambridge University Press, Cambridge, UK, 1964).
[16] W. Shockley, Solid-State Electron. **2**, 35 (1961).
[17] F.S. Lee and Y.C. Cheng, Phys. Rev. B **56**, 6412 (1997).
[18] R.M. Westervelt and S.W. Teitsworth, J. Appl. Phys. **57**, 5457 (1985).
[19] E. Schöll, Phys. Rev. B **34**, 1395 (1986).
[20] K. Kunihiro, M. Gaa, and E. Schöll, Phys. Rev. B **55**, 2207 (1996).
[21] F.-J. Niedernostheide, J. Hirschinger, W. Prettl, V. Novák, and H. Kostial, Phys. Rev. B **58**, 4454 (1998).
[22] V. Novák, J. Hirschinger, F.-J. Niedernostheide, W. Prettl, M. Cukr, and J. Oswald, Phys. Rev. B **58**, 13 099 (1998).
[23] G. Schwarz, C. Lehmann, and E. Schöll, Phys. Rev. B **61**, 10 194 (2000).